American Journal of
Biomedical Science & Research

www.biomedgrid.com
ISSN: 2642-1747

Research Article

Preliminary Computational Studies of Several Estrogen Receptor Modulators

Mindi Buckles[1], T Dwight McGee[2], Jason Ford Green[3], LeeShawn D Thomas[4], Adrian McCollum[4], Adrian Roitberg[2], John Cooperwood[5], Samique March Dallas[6], Jesse Edwards[7] and Jillian Pope[4]*

[1]*Department of Chemistry, Florida A&M University, Tallahassee, Florida, USA*

[2]*Department of Chemistry, College of Liberal Arts and Sciences, University of Florida, Gainesville, Florida, USA*

[3]*Department of Chemistry, Natural Science Division, Bishop State Community College, Mobile, Alabama, USA*

[4]*Department of Biology, College of Science and Technology; Florida A&M University, Tallahassee, Florida, USA*

[5]*Department of Basic Sciences Medicinal Chemistry Division, College of Pharmacy and Pharmaceutical Sciences; Florida A&M University, Tallahassee, Florida, USA*

[6]*Department of Accounting, Finance, and Business Law, School of Business and Industry; Florida A&M University, Tallahassee, Florida, USA*

[7]*Department of Chemistry, School of Computer, Mathematical and Natural Sciences, Morgan State University, Baltimore, USA*

***Corresponding author:** Jillian Pope, Department of Biology, College of Science and Technology; Florida A&M University, Tallahassee, Florida, USA.

To Cite This article: *Mindi Buckles, T Dwight McGee, Jason Ford Green, LeeShawn D Thomas, Adrian McCollum, Adrian Roitberg, John Cooperwood, Samique March Dallas, Jesse Edwards and Jillian Pope*, Preliminary Computational Studies of Several Estrogen Receptor Modulators. Am J Biomed Sci & Res. 2026 30(2) AJBSR.MS.ID.003902,*

DOI: 10.34297/AJBSR.2026.30.003902

Received: February 10, 2026; **Published:** February 23, 2026

Abstract

Endocrine therapy has proven to be an effective treatment for Estrogen Receptor (ER+) positive breast cancer through the disruption of estrogen action. Selective Estrogen Receptor Modulators (SERMs) are a group of compounds that bind to estrogen receptors and elicit agonist or antagonist responses depending on their chemical structure. Tamoxifen is a well-known triphenylethylene SERM that is used as an adjuvant therapy in breast cancer. Based on the stiff steroid fused ring structure of 17-β-Estradiol combined with the amino alkyl-oxy portion of Tamoxifen, *Cooperwood et. al.* [1] synthesized a unique series of steroids with greater or comparable activity to Tamoxifen. We use molecular mechanics to calculate the rotational barriers of the functionalized tails of these estradiol derivatives. In the case of the isopropyl derivative, the barriers around the minimum-energy structure are as low as 10 kcal/mol, while 2 dihedral angles in the amino alkyl-oxy tail are held constant, and the other two are varied from 0 to 360 degrees. This low barrier may enhance the drug's ability to adapt to changes within the active site. It is evident that the majority of the ligands are in their lowest-energy state when dihedral 3 is 180 degrees and dihedral 4 is 300 degrees, except for the piperidine derivative, which attains its minimum energy when dihedral 3 is 180 degrees and dihedral 4 is around 60 degrees. Further investigation of these contour plots and docking studies provides insight into the activity and potential mode of action of these compounds. Docking simulations in AutoDock4.2 reveal specific ligand-amino acid interactions in the binding pocket of the ligand binding domain of the Estrogen Receptor (3ERT) and agree with the interactions found in the 3ERT PDB crystal structure of ER bound to 4HO-tamoxifen. The negative free energies signify that binding is very likely to occur, and the Ki values are indicative that all six estradiol derivatives and 4HO-Tam are possible ligands for ERα.

Introduction

Many environmental factors have been attributed to the development of cancer throughout the body. Compounds included in these factors, Xenoestrogens, are natural or synthetic chemical compounds with structures similar to those of natural estrogens.

One prevalent form of cancer that Xenoestrogens may affect is breast cancer. It has been reported that breast cancer is diagnosed in 1 in 8 women worldwide [2].

Breast cancer is a disease that exhibits great clinical, histopathological, and molecular diversity [3]. Doctors worldwide strive to eradicate breast cancer, and although it has yet to be achieved, significant strides have been made in the treatment and management of the disease. Since the early 1960's, when the first influential molecule in the treatment of breast cancer, the Estrogen Receptor (ER+), was discovered, millions of dollars have been spent on research to determine its structure, function, and importance. Jacobsen and Jensen linked estrogen to the ER in 1962 and demonstrated a positive correlation between the ER docked with estrogen and tumour growth [4,5]. Later, the discovery of Tamoxifen (TAM) marked the first approved endocrine therapy to treat invasive breast cancer, followed by aromatase inhibitors, developed to improve endocrine therapy [6] effectively. There are several issues with endocrine therapy, but perhaps one of the most important is the resistance a patient develops to the treatment. The ER controls the stimulation, proliferation, and differentiation of both cancerous and non-cancerous breast cells. ERs are transcription factors that are activated by ligand binding and can stimulate specific signal transduction pathways involved in breast cancer resistance. (Current research continues in the effort to study the ER+ resistance to better understand, diagnose, and treat breast cancer patients.

Estrogens are steroid hormones secreted into the bloodstream that interact with receptors on target cells, transmitting signals that control the development and maintenance of both female secondary sex characteristics and the female reproductive system. These hormones also help maintain bone mass, support cognitive function, regulate insulin response, and perform many other important functions. Lack of estrogen or estrogen levels can cause many problems, from underdeveloped female secondary sex characteristics to osteoporosis [7]. Estrogen is lipophilic and can easily diffuse across the cell membrane, translocate through the cytoplasm, and bind to specific receptor proteins in the nucleus, activating transcription. The ovaries mainly synthesize estrogen; however, other tissues also manufacture estrogen in smaller quantities [8]. The three estrogens shown in Figure 1 are the most abundant and best-studied natural Estrogen Receptor (ER) agonists, with 17β-Estradiol (E2) acting on ERα (ERα) [9].

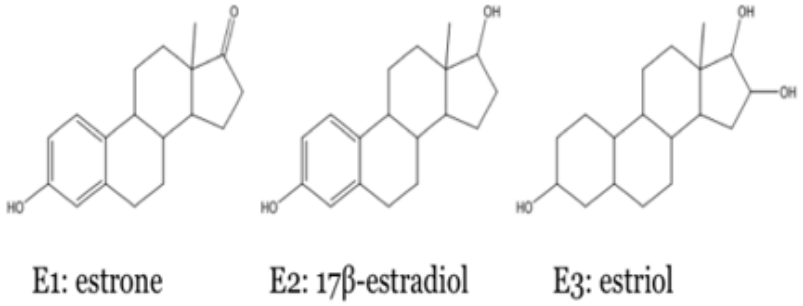

Figure 1: Common endogenous estrogens.

Steroidogenesis for this class of steroids begins in the ovary and is triggered by Follicle-Stimulating Hormone (FSH). Once a signal is received from the FSH, cholesterol is mobilized from the outer to the inner mitochondrial membrane, where the Cytochrome P450 (CYP) 11A enzyme cleaves its side chains to yield pregnenolone. Hydroxysteroid dehydrogenases, hydroxysteroid reductases, and additional CYPs act on pregnenolone and other products, leading to the production of estrogen and other steroid hormones [10]. Ovarian steroidogenesis is depicted in Figure 2.

There are several subtypes of the Estrogen Receptor. The hormones reported in the previous section are the natural binding ligands of the Estrogen Receptor (ER). The ER, a member of the Nuclear Receptor (NR) superfamily of proteins, that ligates to estrogen and causes (modulates) an intracellular response [11]. ERs regulate gene expression upon ligand binding, and the ER undergoes a conformational change that activates or deactivates its mechanism of action. Two subtypes of ERs exist: ER-alpha (ERα) and ER-beta (ERβ). In normal mammary glands, ER expression is stringently controlled and increases during puberty and pregnancy [13]. Figure 3 depicts both ER-α and β- and the percent homology between the two.

All NR proteins are constructed from three domains: the DNA-Binding Domain (DBD), the Ligand-Binding Domain (LBD), and the N-terminal domain, which have similar structures and functions [14]. The DBD and the LBD show high degrees of homology between the two ER subtypes, 97% and 59%, respectively. Given the high degree of relatedness, both subtypes can bind DNA and ligands similarly. The D-domain, known as the hinge region, is necessary for flexibility in both ERs. As the percentages indicate, the most variation is seen in the N-terminal and C-terminal domains, A/B and F. Both Activation Functions (AFs) 1 (AF1) and 2 (AF2) contribute to the sequence in the ERα whereas ERβ only has an AF2

region. Each AF has a distinct role: AF1 induces ligand-independent transcription, while AF2 recruits regulatory coactivators and corepressors to the LBD [15]. For ligand-activated transcription to occur, coregulatory proteins are required to mediate binding between DNA and the ER. Interaction with coregulators occurs at the AF2 site within the LBD, where the hydrophobic pocket formed by helix 12 (H12) recognizes coactivators bearing the LXXLL motif. In the sequence LXXLL, L represents leucine and X any individual amino acid15. E2 binds to the LBD, causing a conformational change in which H12 can close around it, creating a binding site for a coactivator bearing the LXXLL motif [17]. In this case, E2 acts as an agonist for ERα and increases transcriptional activity. Figure 4 shows an agonist, E2, bound to the ERα, allowing for coactivator binding and resulting in increased gene expression.

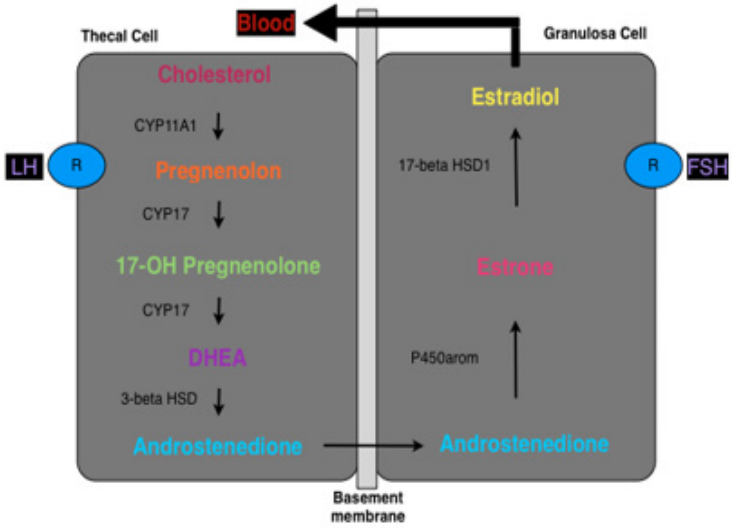

Figure 2: Ovarian steroidogenesis.

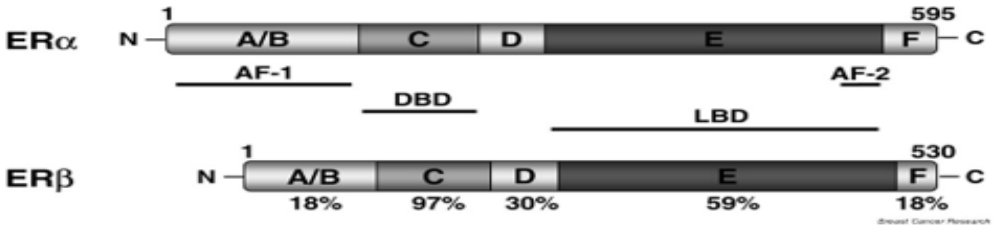

Figure 3: Structure and homology of ER subtypes [12].

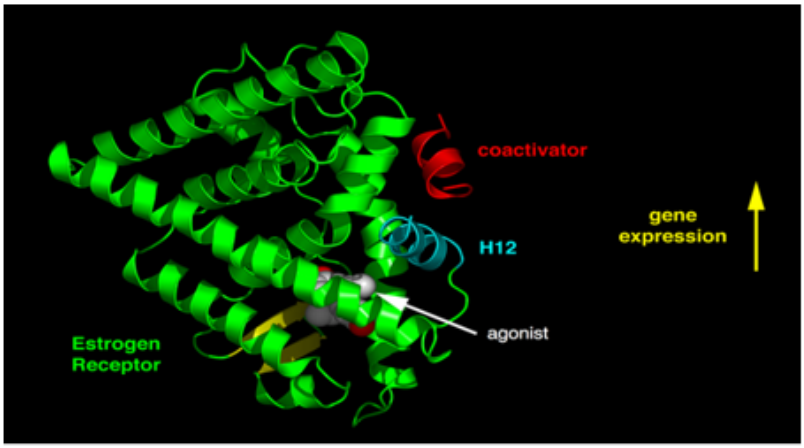

Figure 4: Structural basis for ER agonist action [16].

Ligands with bulky side chains introduce steric hindrance to the hydrophobic binding pocket, leading to a conformational change that prevents H12 from closing. H12 is moved up away from the LBD, making it impossible for a coactivator to bind. This is seen in cases where an antagonist binds to the ERα. Tamoxifen (TAM) is a well-known antagonist that binds to Erα and elicits conformational changes that prevent H12 from closing, ultimately resulting in decreased gene expression. This allosteric effect is depicted in Figure 5 [18].

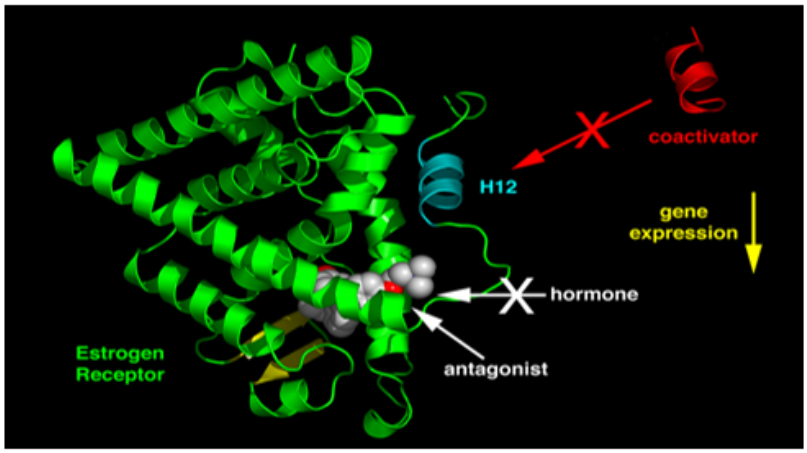

Structural basis for ER antagonist action [16].

ERα and the E2 Response

Before E2 binding, the unbound form of ERα is found bound to the 90 kDa heat shock protein (hsp90) in the cytoplasm of the cell [19]. Hsp90, a chaperone, ensures proper protein folding while bound to the ERα. Hsp90 prevents protein aggregation and binds the immunophilins cyclophilin-40 (CyP40) and peptidyl-prolyl cis-trans isomerase (FKBP52), forming a complex that binds to ERα and guides the activated receptor across the nuclear membrane into the nucleus [20,21]. The dissociation of the hsp90 complex from the ER follows the binding of E2 to ERα and migration into the nucleus. Once hsp90 is detached, the ERα can undergo a conformational change leading to the formation of an ERα homodimer. The Erα dimer, along with coactivators, binds to the Estrogen Response Element (ERE) of the target gene, initiating transcription and cell proliferation [23]. This ERα response to the binding of E2 is illustrated in Figure 6.

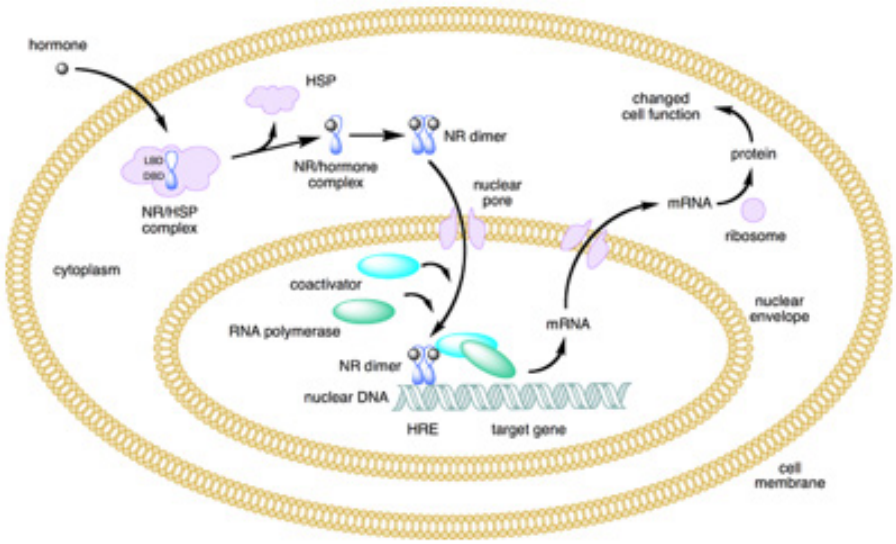

Figure 6: ERα estrogenic response and mechanism for DNA transcription [22].

Selective Estrogen Receptor Modulators (SERMs) have emerged as an attractive target for drug design due to their ability to block 17β-estradiol (E2) from binding to the Estrogen Receptor (ER), thereby reducing the proliferation of estrogen-positive breast cancer cells. Estrogen Receptor Alpha (ERα) has been extensively studied by NMR and crystallography and has been shown to exist in numerous conformations. Helix 12 exhibits the most mobility of all domains, largely attributed to Tryptophan 83 (TRP83). The α-helix remains intact but moves by 13 Å [24] (Figure 7).

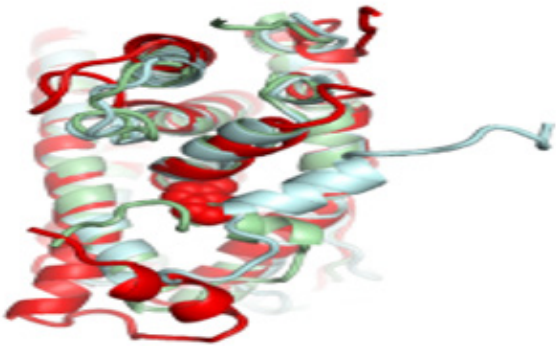

Figure 7: Crystal structure overlay to visualize conformational changes of Helix-12 Blue shows the closed conformation, green shows the open conformation, and red shows the hinge-movement range for Helix-12 [24].

Endocrine therapy has proven to be an effective treatment for estrogen receptor ER+ breast cancer through the disruption of estrogen action. SERMs bind to estrogen receptors and elicit agonist or antagonist responses based on their chemical structure, thereby inducing conformational changes in ERα and ERα. The Cooperwood group synthesized a series of six estradiol derivatives designed with the flexible tail portion of TAM mentioned previously, and a rigid, fused ring portion of E2 to bind to ERα to inhibit breast cancer [25]. This combination is depicted in Figure 8 below.

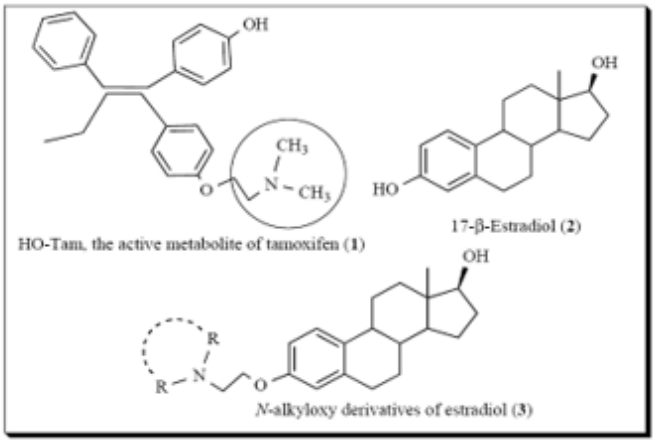

Figure 8: General structure of 4-hydroxy Tamoxifen, 17β-estradiol and *Cooperwood et. al*. estradiol derivatives [25].

There is a wealth of computational research on ERα and E2, but few theoretical studies have been conducted on Cooperwood's unique class of six SERMs. The –R groups in the N-alkyloxy derivatives are ethyl, methyl, pyrrolidine, morpholine, piperidine, and isopropyl functional groups. These E2 derivatives are shown in Figure 9 and are ideally expected to exhibit increased activity and flexibility compared to 4-hydroxytamoxifen (HO-Tam), the active metabolite of TAM [25].

IC50 values indicate the concentration at which 50% of cell growth has been inhibited. These values were measured by Cooperwood, et al., and are presented in Table 1. Indicating increased activity in the diisopropyl and piperidinyl derivatives as compared to that of HO-Tam based upon IC50 values [26,27].

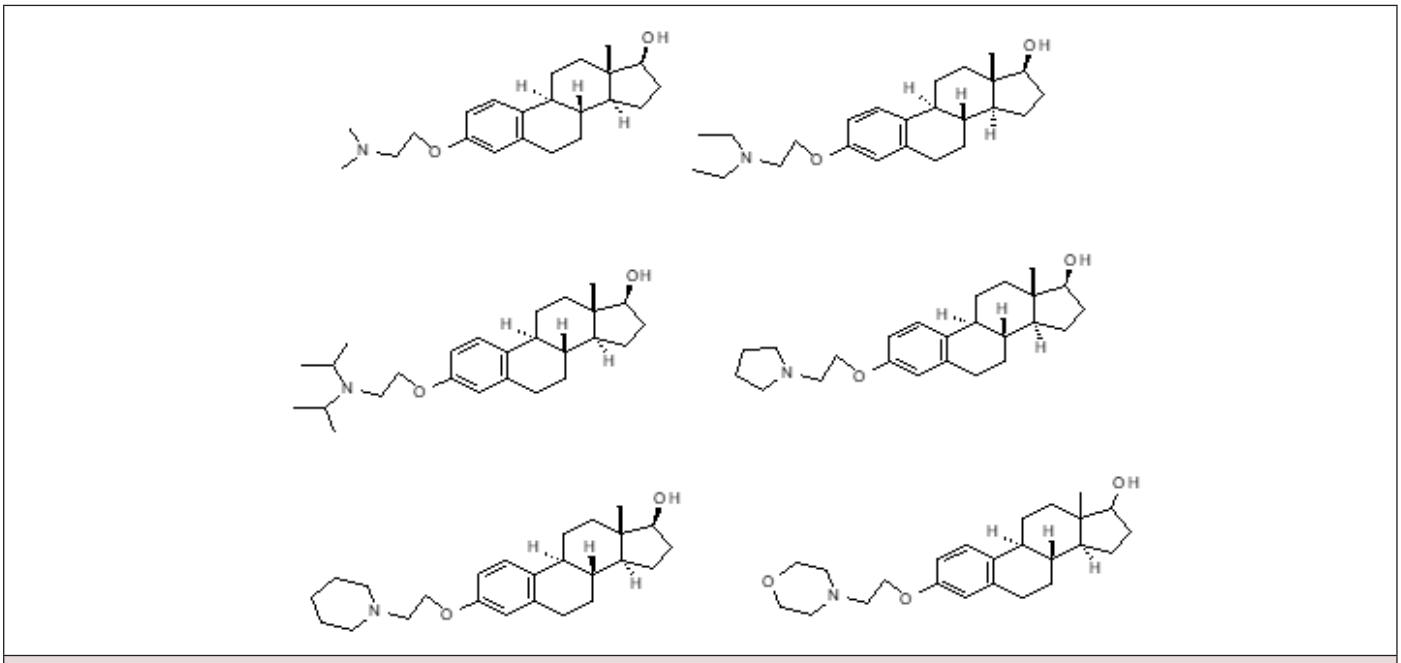

Figure 9: Six estradiol derivatives designed by *Cooperwood, et. al.*, [Beginning at top left and proceeding clockwise: Dimethyl, Diethyl, Pyrrolidine, Morpholine, Piperidine, and Diisopropyl] [25].

Table 1: IC_{50} Values for *Cooperwood, et. al.,* Derivatives and 4-hydroxytamoxifen [25].+

R Group	IC_{50} (μM)
Dimethyl	16.2
Diethyl	8.7
Pyrrolidine Ring	10.8
Morpholine Ring	19.8
Piperidine Ring	4.1
Diisopropyl	5.6
HO-Tam	9

Methods

Molecular Mechanics-derived conformations, Molecular dynamics, molecular docking, and sampling methods were used to determine rotational barriers of the alkyl-oxy-tails described later and to produce geometries necessary for sampling the lowest-energy conformations for docking simulations within the 3ERT ligand-binding domain. Rotational barriers were depicted using potential energy contour plots from conformational searches, each plotted relative to the lowest-energy conformation. Potential energy contour plots were generated using Sybyl 6.9 Software23 to assess the flexibility of this unique class of SERMs. The Molecular Mechanics simulations were run, energies were obtained, and contour plots were created. Since the diisopropyl derivative showed greater activity than HO-Tam, a full profile has been generated to determine whether the N-alkyloxy group is sufficiently flexible. In all contour plots for the analysis of all 6 ligands, the numbering system for the dihedral (torsional) angles is as follows: [28].

Contour plots are graphical representations that are used to map a 3-dimensional potential energy surface through which a molecule can freely rotate. These plots are used to determine flexibility and show energetically favourable conformations when certain dihedral angles are held constant. In all of the contour plots for each ligand, the solid line represents a potential energy of 10 kcal/mol, the dashed line represents 20 kcal/mol; torsional angle 3 is on the x-axis, and torsional angle 4 is on the y-axis. The conformational energies were examined by rotating dihedral angles 1-4 in 60° increments from 0° to 300°. The energy of each conformer is reported in Appendix A of a related work by one of the authors of this work [29].

The Generalized Born Model was used in molecular dynamics simulations to implicitly account for and estimate the free energy of solute-solvent interactions. The Generalized Bohr Model (GB) omits solvent viscosity, and therefore, Langevin Dynamics were used to compensate. Implicit solvation models are used to account for and estimate the free energy of solute-solvent interactions. The Generalized Bohr Model (GB) omits solvent viscosity, so Langevin Dynamics must be used to compensate. In Langevin's motion equations, two force terms have been added to Newton's second law of motion to account for the varying degrees of freedom. Langevin's

equation uses a stochastic differential equation in which the force acting on a particle has three components. Molecular dynamics simulations were conducted using AMBER software.

Cluster analysis was performed using the PTRAJ module of AMBER. A hierarchical algorithm and a root-mean-square value of 2.0 were selected to obtain the highest-frequency low-energy conformers for molecules. A new cluster is created whenever the change exceeds three standard deviations, and the lowest-energy cluster is then used for molecular docking simulations.

Blind docking was performed for each initial and final state of all six ligands using the Lamarckian Genetic Algorithm (LGA). In the initial run, 0.375 Å grid spacing was used. The lowest-energy docked conformation of each ligand was determined and later used in a subsequent docking calculation using a more specific 0.18 Å grid space. The program was set to a maximum of 5 million evaluations, 27,000 generations, a mutation rate of 0.02, and a crossover rate of 0.8. Clustering analysis was used to determine specific docked low-energy conformations. The ligands were prepared with atomic charges fit to reproduce electrostatic potentials and were fit to all ligands, using the Merz-Kollman-Singh method. The preparation was carried out at the B3LYP/cc-pvtz level of theory in the Gaussian09 package. All geometries, binding constants, and intermolecular forces were calculated using the Autodock4.2 program with the AD4 scoring function, and Ki values were calculated using the free energy of binding according to Equation 2-19 below.

$$K_i = e^{(\Delta G/RT)} \qquad (2-19)$$

Equation 2-19 comes from thermodynamics. In this equation, △G represents the free energy of binding, R is the gas constant, and T represents absolute temperature.

Results and Discussion

Contour plots for the diisopropyl derivative show that dihedral angles 1 and 2 are held constant to determine the flexibility and range of the aminoalkyl-oxy tail. Recall, the numbering system is based on Figure 10.

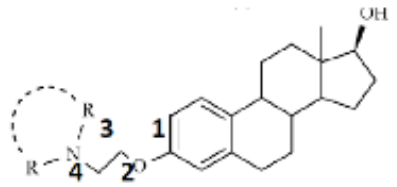

Figure 10: Numbering system for dihedral angles in *Cooperwood, et. al.*, ligands [25].

The contour plots in Figures 11 A-E reveal that when dihedral angle 1 is held constant at 0 degrees, two low-energy channels exist, and dihedral 3 can rotate freely when dihedral 4 is 120 degrees or 300 degrees, while dihedral 2 rests at either 120 degrees, 180 degrees, or 240 degrees. No distinct low-energy channels exist when dihedral angle 2 is held constant at 60 degrees or 300 degrees, while dihedral 1 is held constant at 0 degrees.

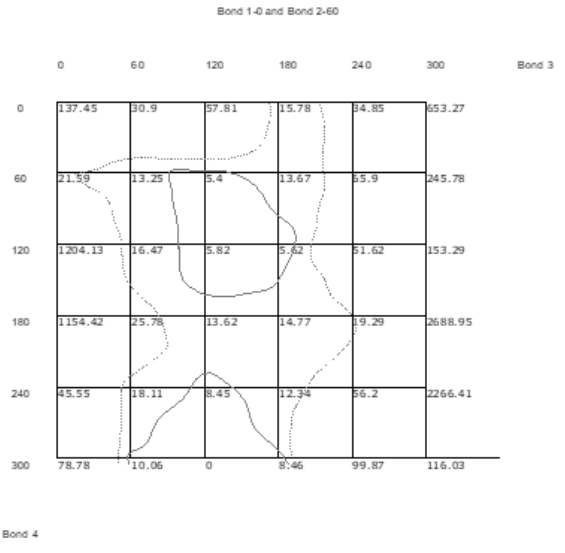

(A)

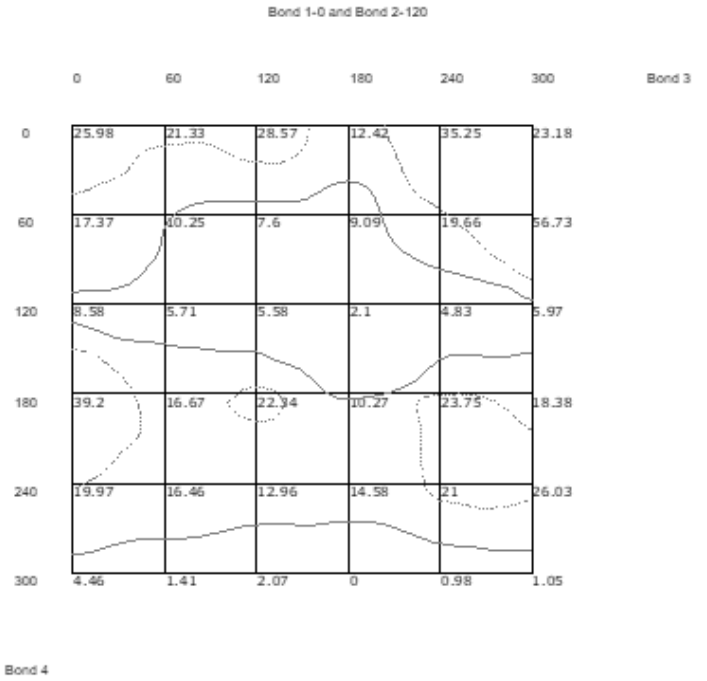
Bond 1-0 and Bond 2-120
0 60 120 180 240 300 Bond 3
0 25.98 21.33 28.57 12.42 35.25 23.18
60 17.37 10.25 7.6 9.09 19.66 56.73
120 8.58 5.71 5.58 2.1 4.83 5.97
180 39.2 16.67 22.34 10.27 23.75 18.38
240 19.97 16.46 12.96 14.58 21 26.03
300 4.46 1.41 2.07 0 0.98 1.05
Bond 4

(B)

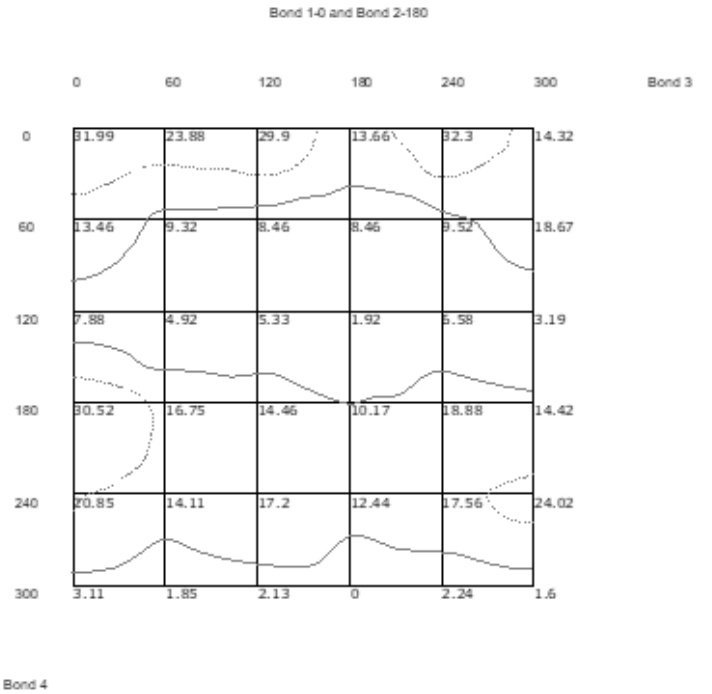
Bond 1-0 and Bond 2-180
0 60 120 180 240 300 Bond 3
0 31.99 23.88 29.9 13.66 32.3 14.32
60 13.46 9.32 8.46 8.46 9.52 18.67
120 7.88 4.92 5.33 1.92 5.58 3.19
180 30.52 16.75 14.46 10.17 18.88 14.42
240 20.85 14.11 17.2 12.44 17.56 24.02
300 3.11 1.85 2.13 0 2.24 1.6
Bond 4

(C)

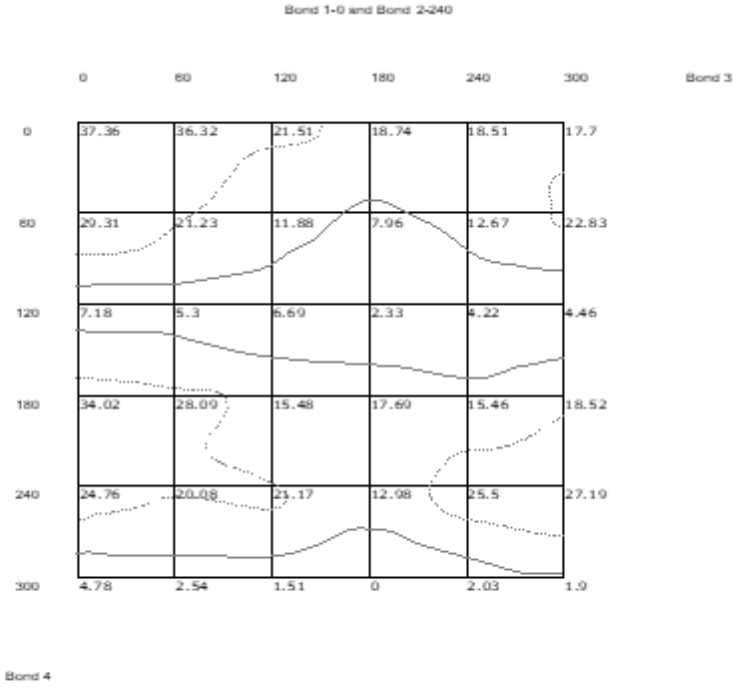

(D)

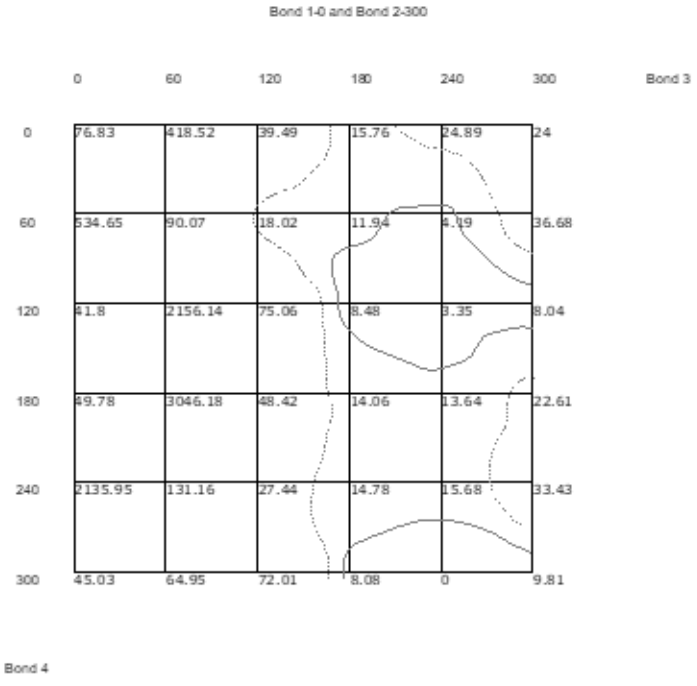

(E)

Figure 11: (A-E) Contour plots of diisopropyl derivative at a dielectric of 1 holding dihedral 1 at 0 degrees and moving dihedral 2 from 60 to 300 degrees.

Figures 12 A-F indicate this ligand can reach various conformations through two main channels: 180 degrees for dihedral 3 and 60 degrees for dihedral 4. When dihedral 2 is held constant at 300 degrees, dihedral 3 is unable to rotate from 0 to 60 degrees. This is evident due to the extremely high potential energy in these regions, ranging from 73.54 kcal/mol to nearly 3,000 kcal/mol. Ligand rotations cannot overcome this energy barrier. Similar energies exist in Figure 11-E when dihedral 2 is held at 300 degrees. The majority of the conformations depicted in Figures 11 A-E have significant energy barriers for dihedral 3 at 0 degrees. These barriers are likely caused by steric hindrance between the isopropyl side chains and the fused steroid ring system.

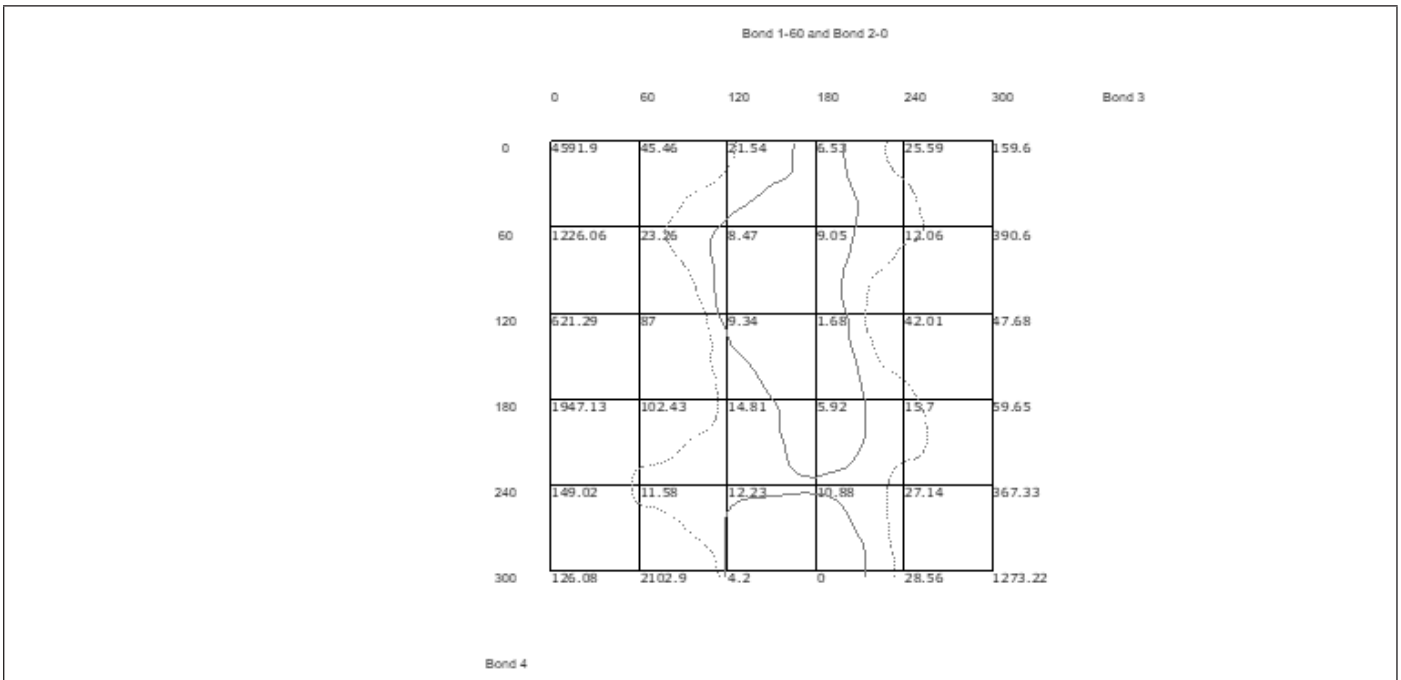

(A)

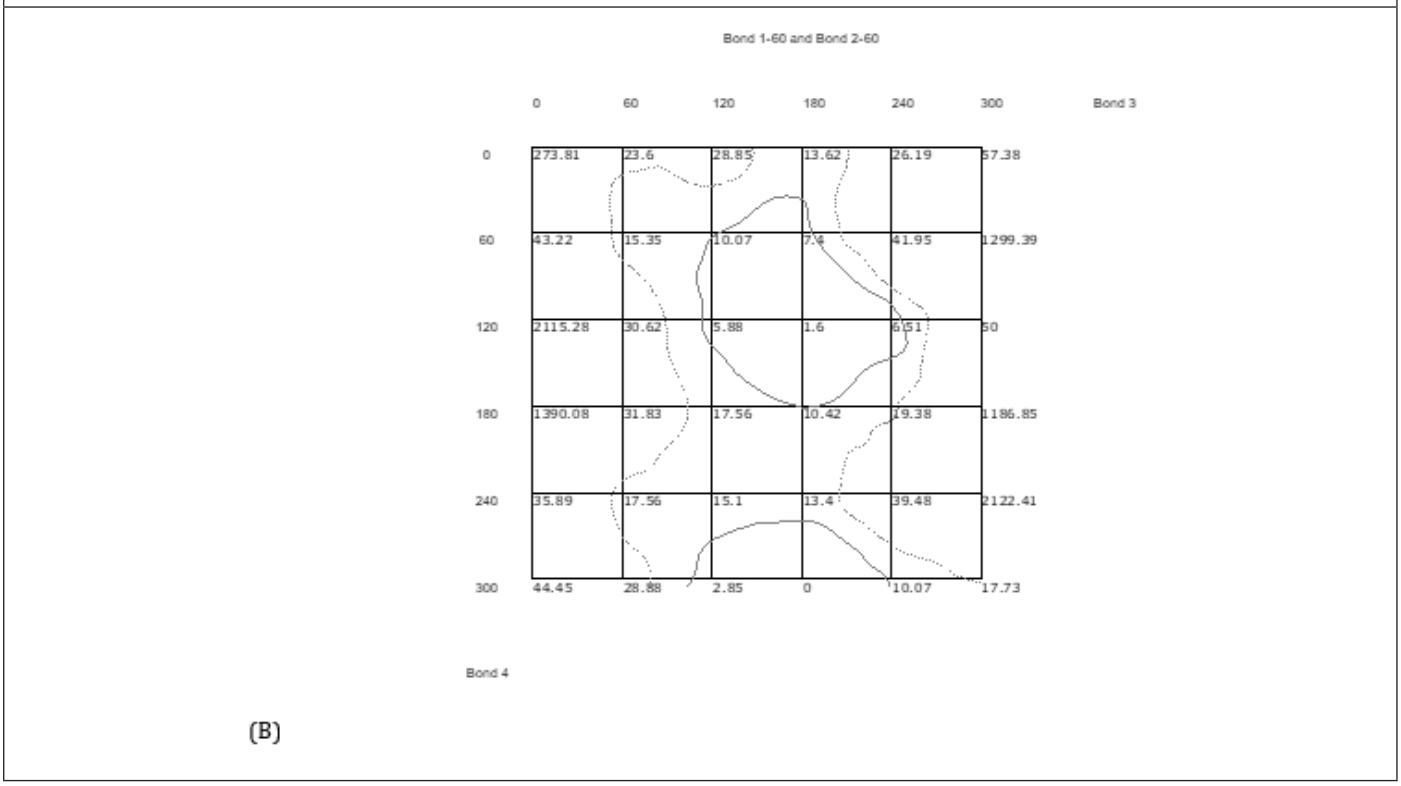

(B)

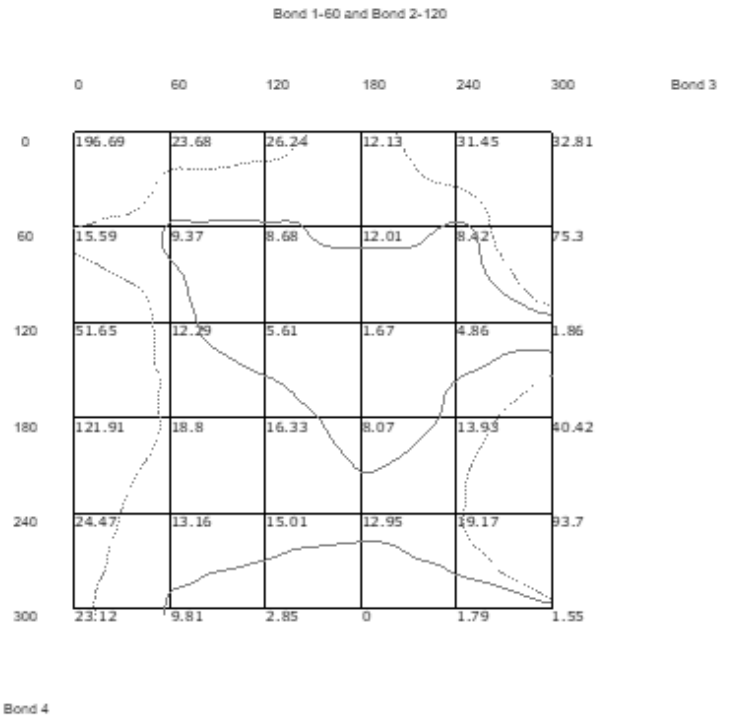
Bond 1-60 and Bond 2-120
0
60
120
180
240
300
Bond 3
196.69
23.68
26.24
12.13
31.45
32.81
15.59
9.37
8.68
12.01
8.42
75.3
51.65
12.29
5.61
1.67
4.86
1.86
121.91
18.8
16.33
8.07
13.93
40.42
24.47
13.16
15.01
12.95
19.17
93.7
23.12
9.81
2.85
0
1.79
1.55
Bond 4

(C)

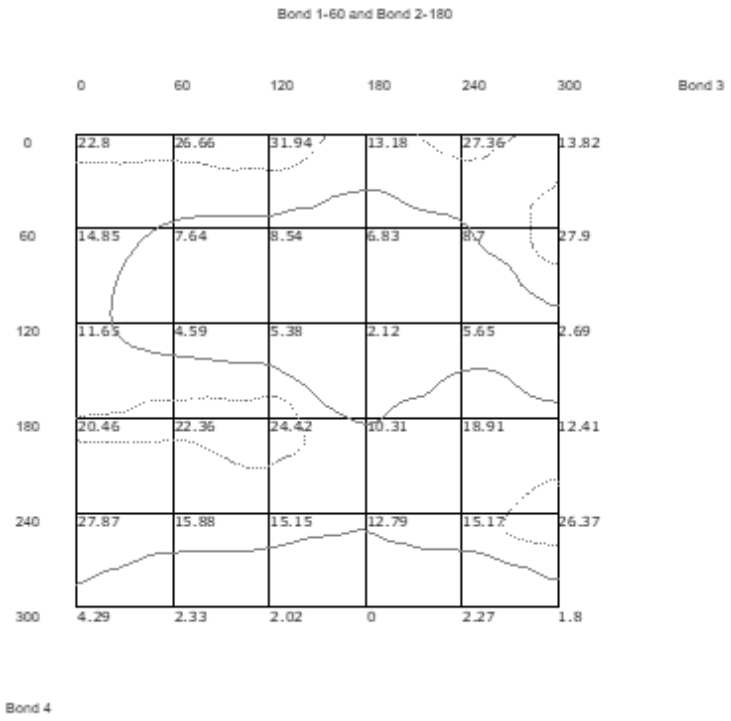
Bond 1-60 and Bond 2-180
0
60
120
180
240
300
Bond 3
22.8
26.66
31.94
13.18
27.36
13.82
14.85
7.64
8.54
6.83
8.7
27.9
11.65
4.59
5.38
2.12
5.65
2.69
20.46
22.36
24.42
10.31
18.91
12.41
27.87
15.88
15.15
12.79
15.17
26.37
4.29
2.33
2.02
0
2.27
1.8
Bond 4

(D)

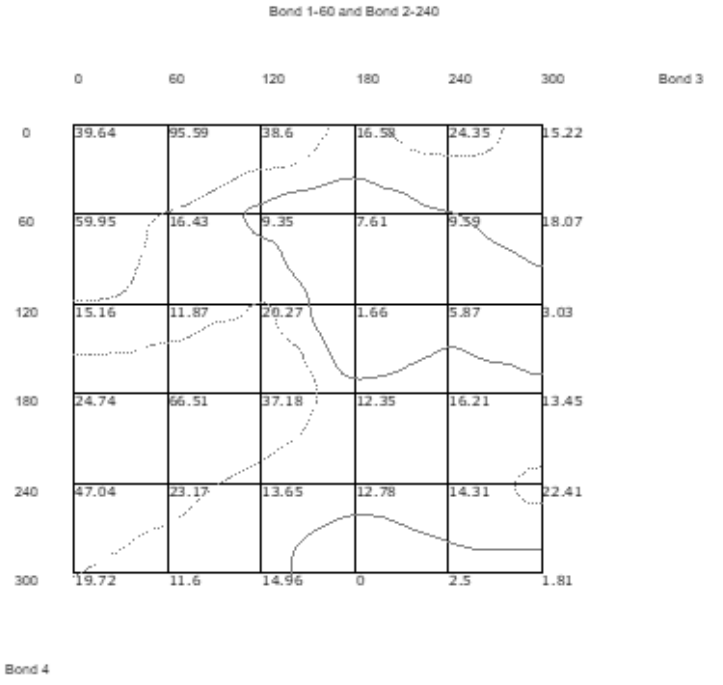

(E)

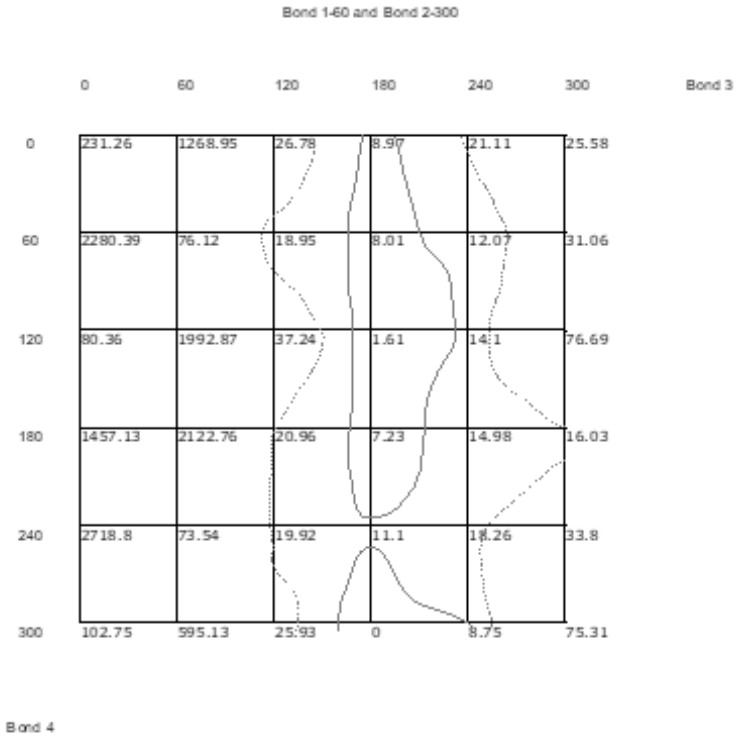

(F)

Figure 12: (A-F) Contour plots of diisopropyl derivative at a dielectric of 1 holding dihedral 1 at 60 degrees and moving dihedral 2 from 0 to 300 degrees.

Similar results are obtained to those in Figures 12 (A-F) when holding dihedral 1 constant at 120 degrees. Each corresponding dihedral angle shows nearly identical contour lines at 10 kcal/mol and 20 kcal/mol. The lowest-energy conformer of diisopropyl is found when dihedral angles 1 and 2 are 120 degrees, with torsional angles 3 and 4 at 180 and 300 degrees, respectively. Additionally, this is the case for all contour plots in Figures 11-13, except plot 11-E, which differs only by a 60° torsional rotation about bond 3.

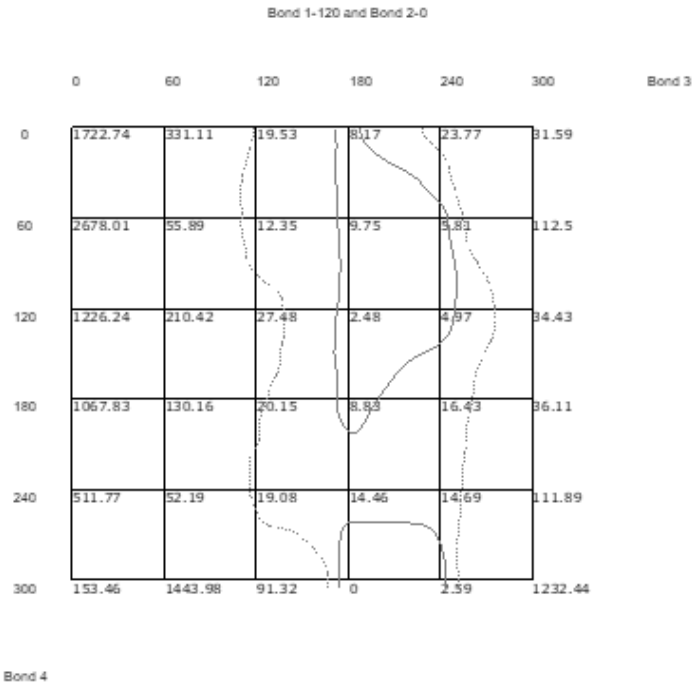

(A)

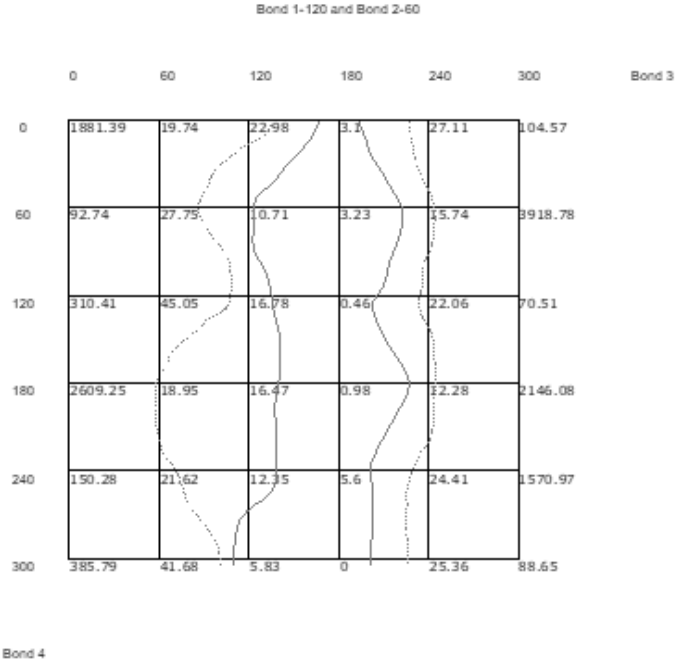

(B)

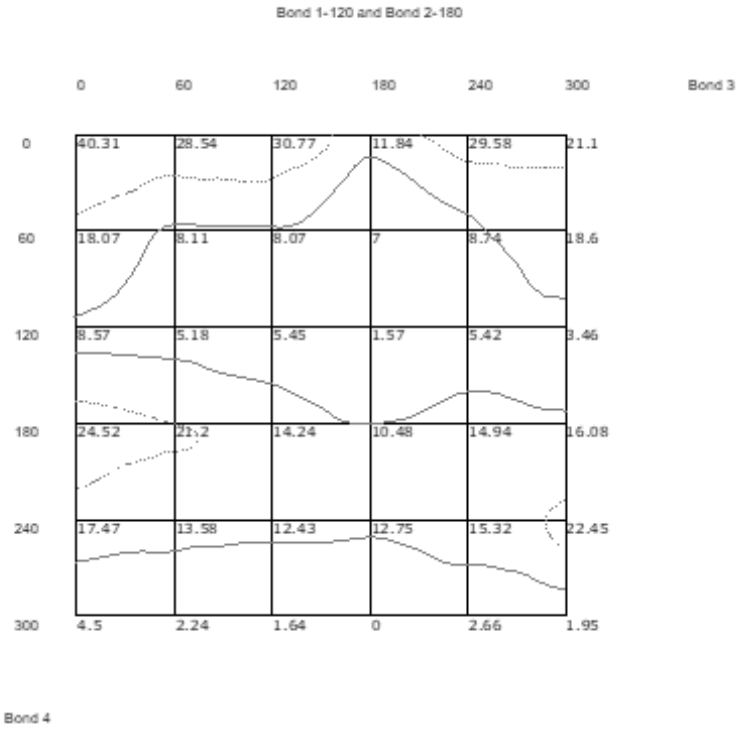
Bond 1-120 and Bond 2-180
0
60
120
180
240
300
Bond 3
40.31
28.54
30.77
11.84
29.58
21.1
18.07
8.11
8.07
7
8.74
18.6
8.57
5.18
5.45
1.57
5.42
3.46
24.52
21.2
14.24
10.48
14.94
16.08
17.47
13.58
12.43
12.75
15.32
22.45
4.5
2.24
1.64
0
2.66
1.95
Bond 4

(C)

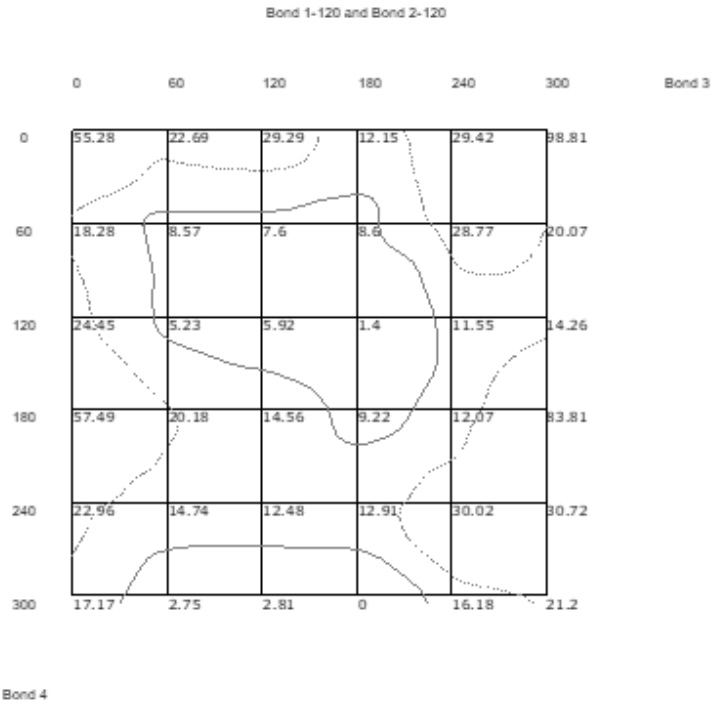
Bond 1-120 and Bond 2-120
0
60
120
180
240
300
Bond 3
55.28
22.69
29.29
12.15
29.42
98.81
18.28
8.57
7.6
8.6
28.77
20.07
24.45
5.23
5.92
1.4
11.55
14.26
57.49
20.18
14.56
9.22
12.07
83.81
22.96
14.74
12.48
12.91
30.02
30.72
17.17
2.75
2.81
0
16.18
21.2
Bond 4

(D)

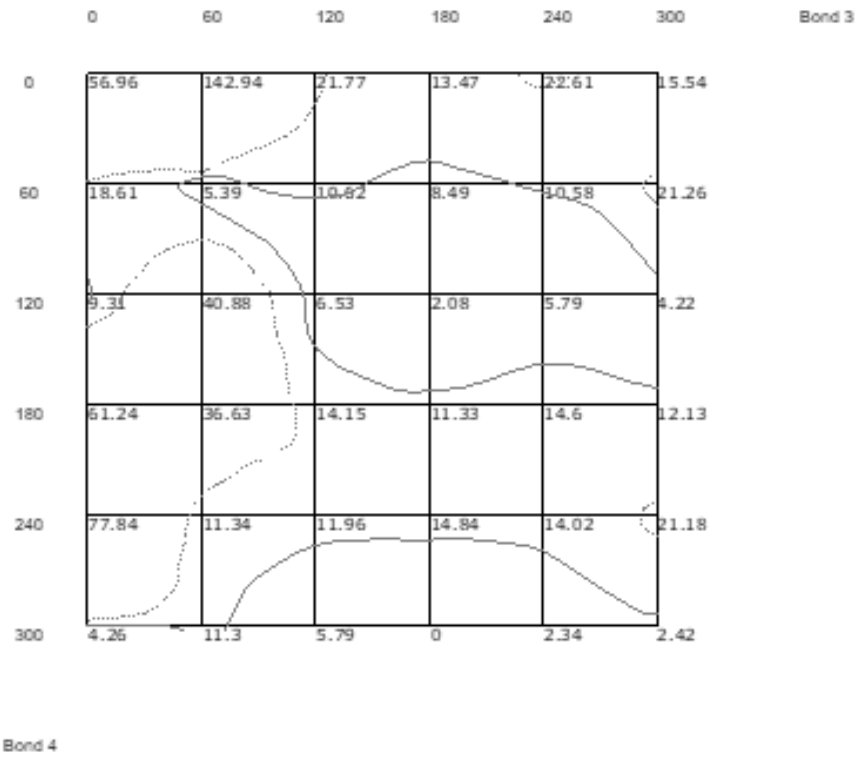

(E)

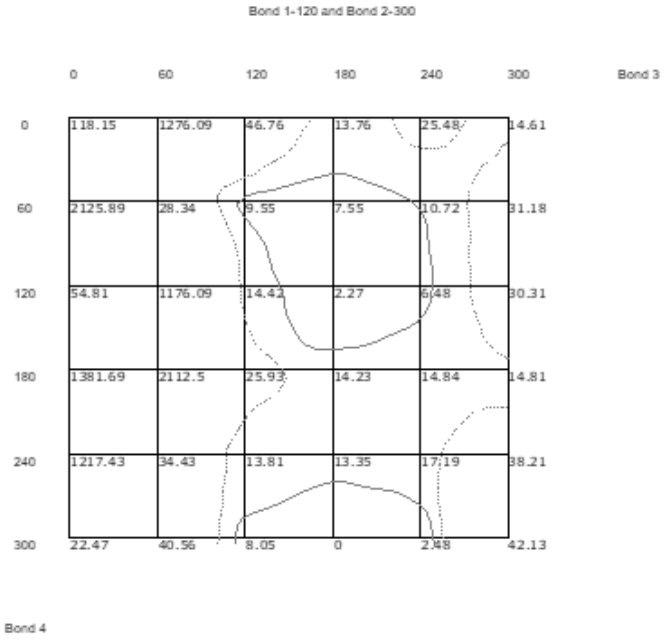

(F)

Figure 13: (A-F) Contour plots of diisopropyl at a dielectric of 1, holding dihedral 1 constant at 120 degrees and moving dihedral 2 from 0 to 300 degrees.

Figures 14 (A-E) show results nearly identical to those in Figures 11-13, consistently pointing to increased flexibility through two main channels: 180 degrees for dihedral 3 and 120 degrees for dihedral 4. Holding dihedral 2 at 300 degrees prevents dihedral 3 from rotating freely from 0 to 120 degrees. The large potential energy in these regions, ranging from 20.71 to nearly 3,000 kcal/mol, accounts for the lack of mobility of the amino-alkyl-oxy tail portion of the ligand. This energy barrier suggests that it is highly unlikely to find the isopropyl derivative obtaining a geometry with the third dihedral angle between 0 degrees and 120 degrees.

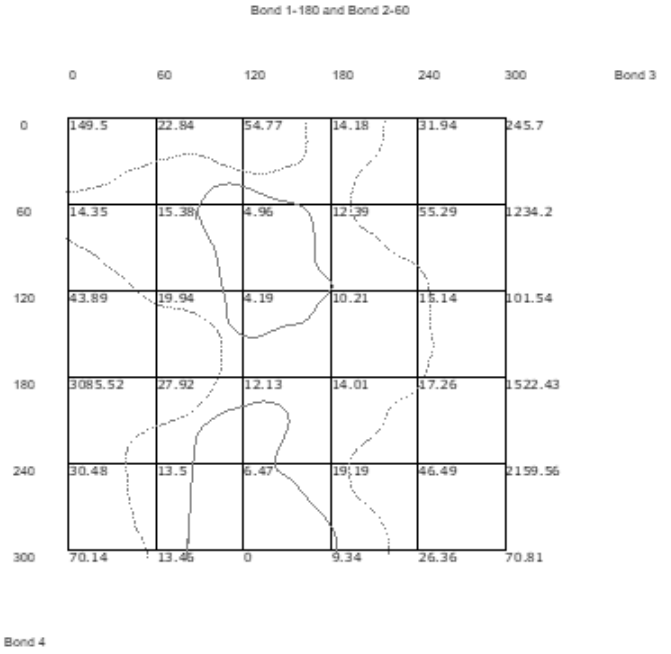

(A)

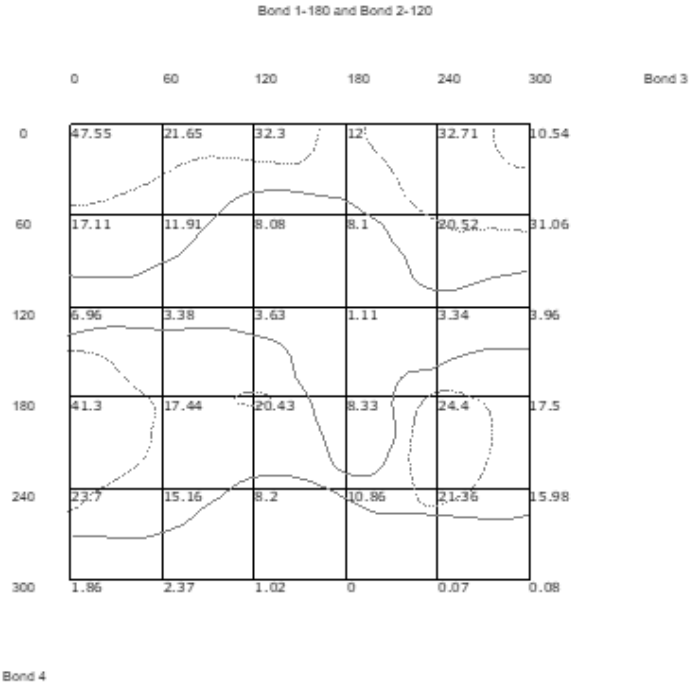

(B)

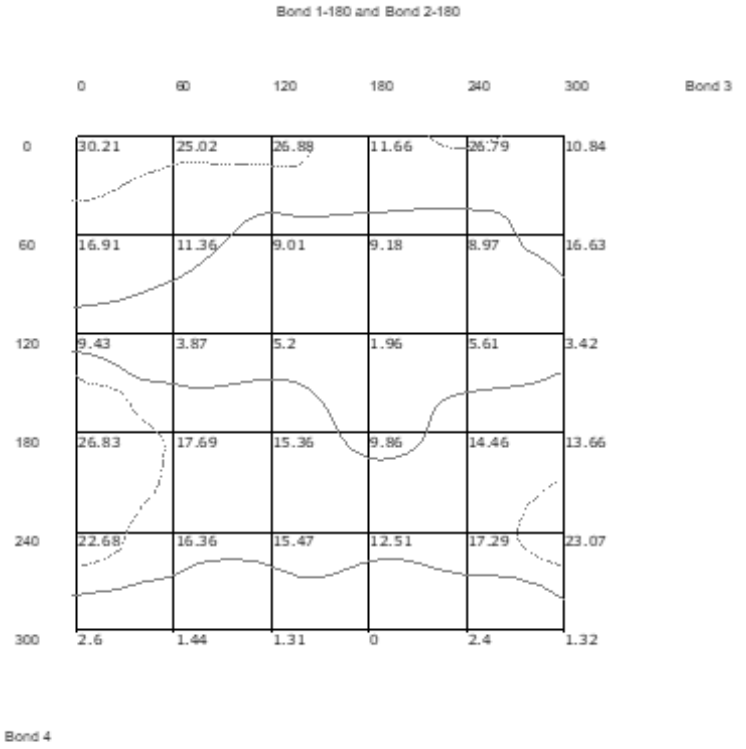
Bond 1-180 and Bond 2-180
0 60 120 180 240 300 Bond 3
0 30.21 25.02 26.88 11.66 26.79 10.84
60 16.91 11.36 9.01 9.18 8.97 16.63
120 9.43 3.87 5.2 1.96 5.61 3.42
180 26.83 17.69 15.36 9.86 14.46 13.66
240 22.68 16.36 15.47 12.51 17.29 23.07
300 2.6 1.44 1.31 0 2.4 1.32
Bond 4

(C)

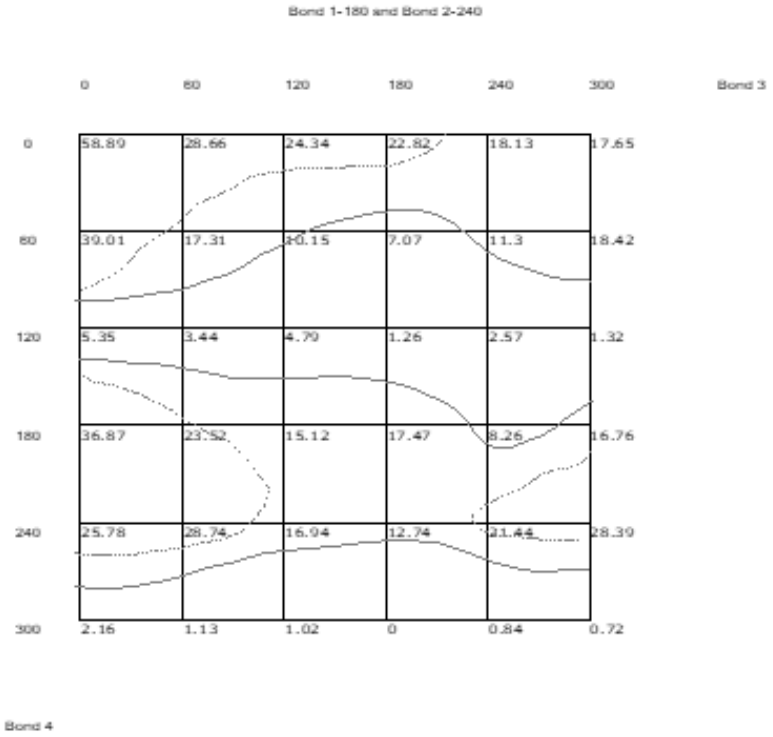
Bond 1-180 and Bond 2-240
0 60 120 180 240 300 Bond 3
0 58.89 28.66 24.34 22.82 18.13 17.65
60 30.01 17.31 10.15 7.07 11.3 18.42
120 5.35 3.44 4.79 1.26 2.57 1.32
180 36.87 23.52 15.12 17.47 8.26 16.76
240 25.78 28.74 16.04 12.74 21.44 28.39
300 2.16 1.13 1.02 0 0.84 0.72
Bond 4

(D)

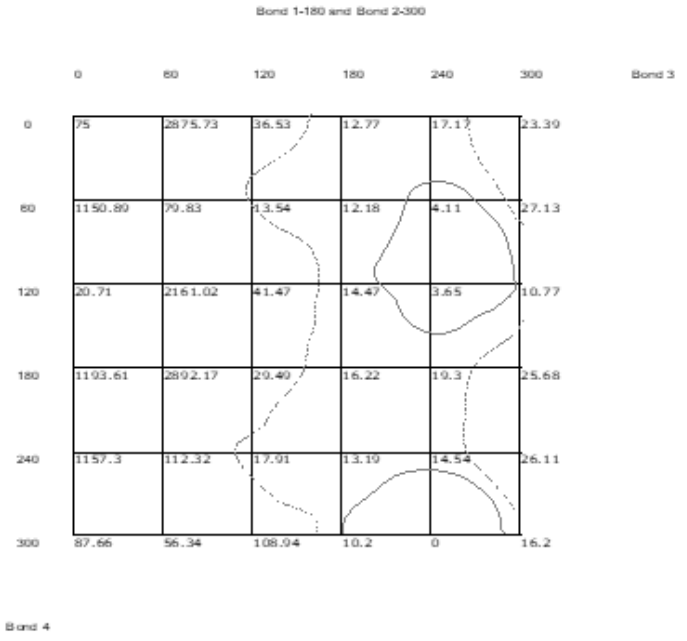

(E)

Figure 14: (A-E) Contour plots of diisopropyl derivative at dielectric 1 holding dihedral 1 at 180 degrees and moving the dihedral from 2 through 60 to 300 degrees.

Low-Energy Conformers for All Cooperwood, et. al., Derivatives

The basic geometry of each ligand may be classified by the torsion of the four dihedral angles throughout each ligand. The lowest-energy state leads to a favourable energetic conformation. This is the likely conformation the ligand will adopt in the absence of intermolecular forces. In these simulations, protein-ligand interactions are disregarded, and MD simulations are carried out at a dielectric constant of 1 (vacuum). The 5 lowest energy conformers have been determined for each ligand, and their conformation, torsional arrangement, and relative energies are provided in Table 2 (A-F).

Tables 2: (A-F) Lowest Energy Conformations for *Cooperwood, et. al.*, Ligands.

Ligand Conformation	Torsional Arrangement D1-D2-D3-D4	Relative Energy (kcal/mol)
1221	120-300-180-300	0
1224	300-300-180-300	0.309
1196	60-60-180-300	0.352
1199	240-60-180-300	0.470
1207	0-180-180-300	0.911

(A) Diisopropyl.

Ligand Conformation	Torsional Arrangement D1-D2-D3-D4	Relative Energy (kcal/mol)
1199	240-60-180-300	0
1221	120-300-180-300	0.021
1207	0-180-180-300	0.121
1196	60-60-180-300	0.128
1224	300-300-180-300	0.177

(B) Dimethyl.

Ligand Conformation	Torsional Arrangement D1-D2-D3-D4	Relative Energy (kcal/mol)
1005	120-300-180-240	0
0983	240-60-180-240	0.015
0991	0-180-180-240	0.070
1199	240-60-180-300	0.135
1207	0-180-180-300	0.0268

(C) Diethyl.

Ligand Conformation	Torsional Arrangement D1-D2-D3-D4	Relative Energy (kcal/mol)
1199	240-60-180-300	0
1221	120-300-180-300	0.042
1207	0-180-180-300	0.208
1224	300-300-180-300	0.266
1196	60-60-180-300	0.285

(D) Pyrrolidine.

Ligand Conformation	Torsional Arrangement D1-D2-D3-D4	Relative Energy (kcal/mol)
1199	240-60-180-300	0
1221	120-300-180-300	0.053
1207	0-180-180-300	0.171
1224	300-300-180-300	0.324
1196	60-60-180-300	0.325

(E) Morpholine.

Ligand Conformation	Torsional Arrangement D1-D2-D3-D4	Relative Energy (kcal/mol)
0343	0-180-180-60	0
0357	120-300-180-60	0.025
0335	240-60-180-60	0.117
0332	60-60-180-60	0.126
0360	300-300-180-60	0.177

(F) Piperidine.

Tables 2 A-F provide significant energetic data, namely the trend in every dihedral angle 3 for each ligand being firm at 180 degrees for all minimum energy conformers. Except for the piperidine derivative, the lowest-energy conformations are found when dihedral 4 is around 300 degrees. Piperidine hits its minimum energy state when dihedral 4 is near 60 degrees. Based on the data from Tables 2 A-F, it is evident that the majority of the ligands are in their lowest energy state when dihedral 3 is 180 degrees and dihedral 4 is 300 degrees. With this in mind, the flexibility of bonds 1 and 2 was analyzed while dihedrals 3 and 4 were held constant at these low-energy angles, and the following information was obtained.

In the diisopropyl derivative, the system was relatively rigid when dihedral 2 was at 0 degrees. However, diisopropyl shows increased flexibility and potential for movement of the isopropyl tail across all dihedral 1 values when dihedral 2 is 120, 180, or 240 degrees. There are slight barriers present when dihedral 2 is 300 degrees, ranging from 0 to 16.7 kcal/mol. Still holding dihedrals 3 and 4 constant at 180 and 300 degrees, respectively, shows energy barriers exist in all conformations of the dimethyl derivative where dihedral 1 is 180 degrees (ranging from 10.061 to 58.314 kcal/

mol) as well as all conformations where dihedral 2 is 0 degrees (ranging from 10.460 to 58.314 kcal/mol); except when dihedral 1 is 300 degrees and dihedral 2 is 0 degrees, for which no rotational barriers were detected.

The energetics for the diethyl derivative were determined using two different sets of bond angles due to the lowest energy conformations found in Tables 2A-F, showing minima when dihedral 4 is at 240 and 300 degrees with dihedral 3 at 180 degrees. Holding dihedral 3 at 180 degrees and dihedral 4 at 240 degrees, energy barriers exist when dihedral 1 is 180 degrees for all possible values of dihedral 2 except when it is 180 degrees. These barriers go up to 58.312 kcal/mol. Another barrier, albeit very small (up to 11.9 kcal/mol), is observed when dihedral 1 is 240 degrees and dihedral 2 is around 0 or 300 degrees. Holding dihedral 4 at 300 provided information indicating that energy barriers of up to 50.793 kcal/mol exist in all conformations where dihedral 2 is 0 degrees, except when dihedral 1 is at 300 degrees. No energy barriers were detected when dihedral 2 is 180, with energy values ranging from 0.268 to 1.063 kcal/mol. Only small rotational barriers, up to 13.231 kcal/mol, exist for these conformations when dihedral 1 is 180 degrees and dihedral 2 is 240 degrees. At all other angles, dihedrals 1 and 2 can rotate freely.

The morpholine derivative was found to have great flexibility, with little or no rotational barriers, ranging from 0.750 to 1.341 kcal/mol, for dihedral 1 when dihedrals 2, 3, and 4 are 180, 300, and 300 degrees, respectively. This derivative, like the diisopropyl, dimethyl, and diethyl derivatives, also experienced a low energy state when dihedral angle 3 is 180 degrees and dihedral 4 is 300 degrees, yielding a free range of torsional motion in all directions except when dihedral 2 is 0 degrees. Also, when dihedral 3 is 180 degrees and dihedral 4 is 300, the pyrrolidine derivative has rotational barriers only when dihedral 1 is 180 degrees or dihedral 2 is 0 degrees.

Deviating from the pattern, the piperidine derivative does not exhibit low energy at a dihedral angle of 300 degrees. Instead, the low-energy conformers of this ligand were found when dihedral 3 is 180 degrees and dihedral 4 is around 60 degrees. In this arrangement, the piperidine ring moves fluidly except when dihedral 2 is 0 degrees. This deviation of dihedral 4 is likely due to the lack of a free electron-withdrawing group in the piperidine derivative. The other 5 ligands have more accessible electron-withdrawing groups. In the dimethyl, diethyl, and diisopropyl derivatives, the R groups may slightly sterically hinder the electron-withdrawing action of the nitrogen, but these R groups have greater flexibility than a ring attachment. The morpholine and pyrrolidine derivatives both have a ring system that allows electron density to be spread out and, therefore, more accessible for electron-withdrawing action. Pyrrolidine's nitrogen is conjugated to the attached ring so that electron density can spread across the ring. The morpholine derivative has two electron-withdrawing groups: a nitrogen on one side of the ring and an oxygen on the other. In all cases, for the piperidine derivative, when dihedral 3 is 180 degrees, dihedral 4 is 180 degrees, and dihedral 1 is 240 or 300 degrees, dihedral 2 has minimal rotational barriers, ranging from 0.290 to 12.137 kcal/mol.

In the majority of cases, a large energy barrier was present for each ligand when the dihedral angle 2 reached 0 degrees. This conformation most likely has the greatest intramolecular steric hindrance, causing unfavourable potential energy and ultimately leading to rotational barriers.

Clustering analysis was carried out to identify the most frequent low-energy conformations, yielding the graph shown in Figure 15. The lowest-energy cluster for each ligand was docked to ERα using AutoDock4.2. Ki values for each ligand-protein complex were obtained, and the Gibbs free energy of binding was calculated. Ki values indicate the binding affinity between a ligand and a protein but provide no information on a ligand's biological potency or activity. Ki values provide insight into whether a molecule can act as a ligand for a specific receptor and describe the strength of protein-ligand interactions.

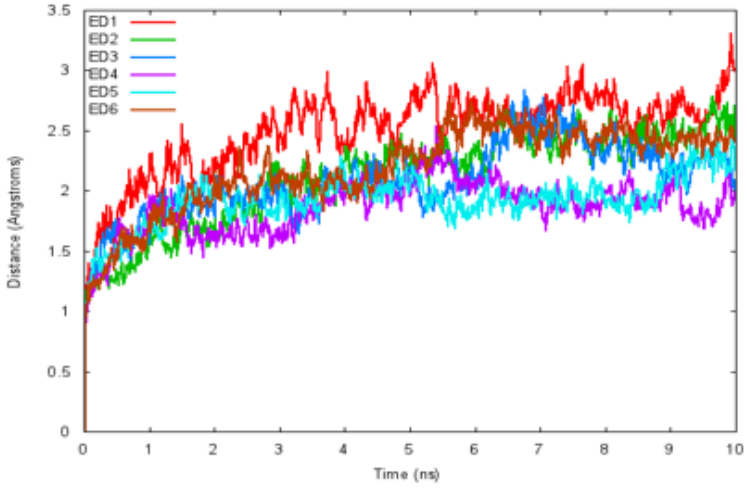

Figure 15: Cluster analysis [1] estradiol derivatives.

To verify a successful docking, the crystal structure for 3ERT [the accepted molecular structure of 4-hydroxytamoxifen (4HO-Tam) complexed with Erα] from the Protein Data Bank (PDB) was used to compare interacting amino acid residues in the ligand binding domain (LBD)73. The images in Figure 16 were created using the RCSB PDB Ligand Explorer 4.0 and the 3ERT crystal structure. In each picture, interacting ERα residues within 4 Å of the 4HO-Tam are labelled. The surface shown in Figure 3.10 shows the hydrophobic binding pocket, with the amino-alkyl-oxy tail of 4HO-Tam protruding from it in Figure 16 B. It has been proposed that the flexibility of the exposed tail leads to a conformational change in ERα that blocks H12 closure, eliciting an antagonistic effect and thereby decreasing ERα17 gene expression.

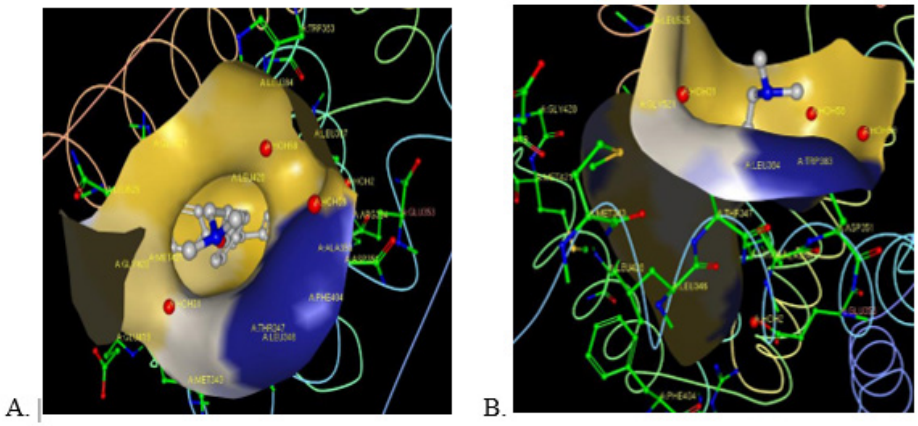

Figure 16: Visual representation of 3ERT using RCSB PDB Ligand Explorer 4.0 A. Shows surface of hydrophobic binding pocket; B. Shows amino-alkyl-oxy tail sticking out of the hydrophobic binding pocket.

RCSB PDB Ligand Explorer 4.0 software was also used to visualize more detailed interactions between Erα amino acid residues and 4HO-Tam, yielding Figure 17.

Using AutoDock4.2, each low-energy cluster was docked, and the images in Figure 18 A-F were obtained. For each docked derivative examined in this work, the Erα amino acid residues are offset by 305 units, and some of the closest interactions are color-coded within Figure 17 to show corresponding amino acid residues indicative of successful molecular docking. There are additional common residues in Figures 17 and 18; however, only a few are highlighted.

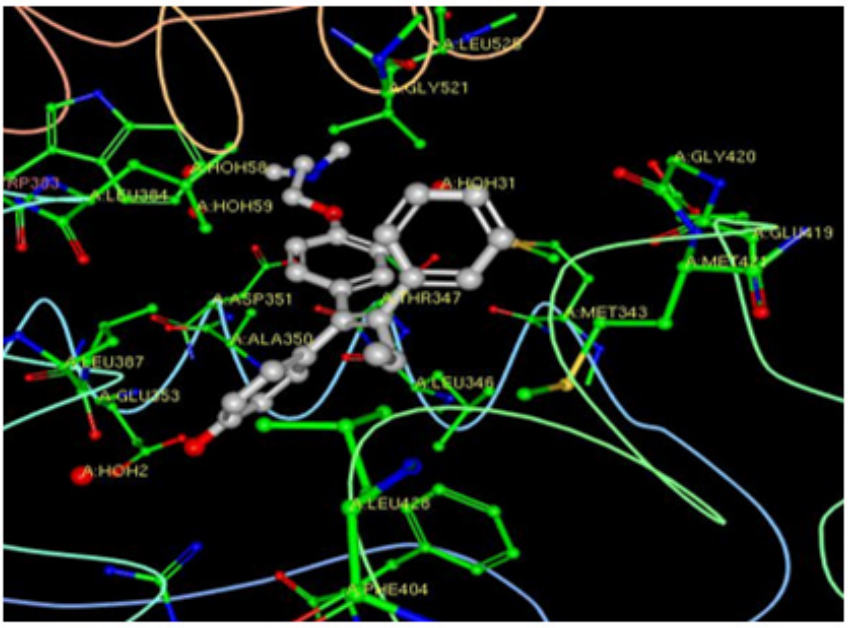

Figure 17: Interacting Erα amino acid residues within 4 Å of the 4HO-Tam.

In addition to the docked structures from Figures 18 A-F, Ki values and free energies were also calculated. Table 3 shows both the Ki values and free energies for all 6 ligands and 4HO-Tam, as determined by AutoDock4.2 molecular docking simulations68.

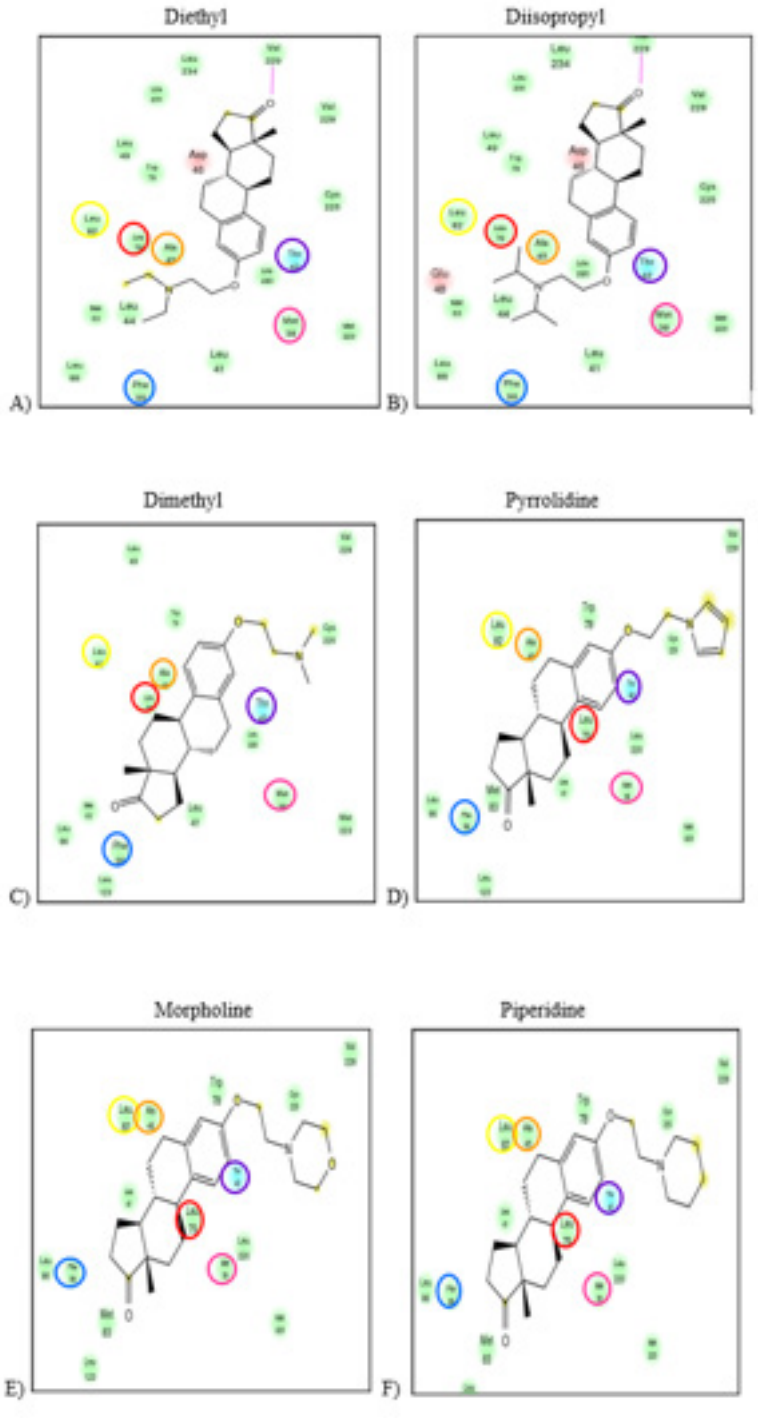

Figure 18: (A-F) Coordination of [1] estradiol derivatives in Erα LBD.

Table 3: Binding energies and K_i values from AutoDock4.2.

Ligand	K_i (μM)	Gibb's Free Energy of Binding (kcal/mol)
4HO-TAM	752.35	-4.26
Diethyl	91.24	-5.51
Diisopropyl	755.13	-4.26
Dimethyl	31.31	-6.14
Pyrrolidine	18.17	-6.47
Morpholine	33.65	-6.1
Piperidine	11.12	-6.76

The negative binding energies calculated in AutoDock4.2 indicate that binding does occur, and the Ki values also suggest that all of the docked molecules are structurally suitable ligands for the ERα protein. Two data points to note are those for 4-HOTam and the diisopropyl derivative. Both have much higher Ki values than the other ligands, which correlate with lower IC50 values.

Figure 19 shows the free energy of binding versus experimental IC50 values for the six [1] estradiol derivatives, as well as 4-HOTam. There is no trend between the experimentally determined IC50 values and the free energy of binding calculated in AutoDock4.2.

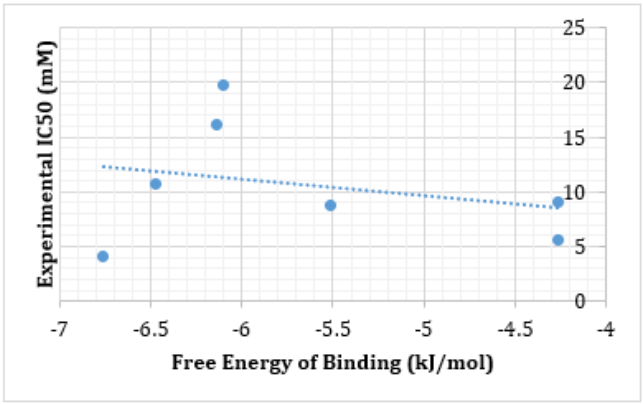

Figure 19: Free Energy of Binding versus Experimental IC50.

Conclusions

From the above results, one could propose that [1] synthesized a unique series of six estradiol derivatives with greater or comparable activity to Tamoxifen based on conformational analysis and molecular docking simulations. Rotational barriers of the functionalized tails of these estradiol derivatives indicate great flexibility for all six ligands. For the isopropyl derivative, the barriers around the minimum-energy structure are as low as 10 kcal/mol, and it is evident that the majority of the ligands are in their lowest-energy state when dihedral angle 3 is 180 degrees and dihedral angle 4 is 300 degrees. Piperidine is the exception, hitting its minimum energy state when the dihedral angle 4 is around 60 degrees. The results also suggest that the derivatives studied in this work exhibit similar properties in their ability to block the binding pocket of 3ERTα, and that all ligands have a flexible end similar to 4HO-Tam. In particular, docking simulations in AutoDock4.2 reveal specific ligand-protein interactions in the binding pocket of the LBD of the estrogen receptor (3ERT) and agree with the interactions found in the 3ERT PDB crystal structure bound with 4HO-tamoxifen. The negative free energies signify that binding is very likely to occur, and the Ki values are indicative that all six estradiol derivatives and 4HO-Tam are possible ligands for ERα.

Acknowledgements

This work was supported in part by the Department of Biology and Chemistry Title III programs at Florida A&M University, the NOAA Educational Partnership Program (EPP)-NOAA Environmental Cooperative Science Center (ECSC) Cooperative Agreement #NA11SEC4810001, and the National Institutes of Health RCMI program grant number G12 RR 03020.

The authors of this work would like to extend their sincere appreciation to the Florida A&M University School of Graduate

Studies, the Department of Chemistry, and Morgan State University for their support.

References

1. John S Cooperwood, Jesse Edwards, Musiliyu Musa, Devora Simmons, Abdul D Mian, et al. (2010) Synthesis and evaluation of estradiol derivatives as anti-breast cancer agents. Letters in Drug Design & Discovery 7(6): 389-394.
2. *http://www.ncbi.nlm.nih.gov/pubmedhealth/PMH0001911/.*
3. Weigelt Britta, Jorge S Reis Filho (2009) Histological and molecular types of breast cancer: is there a unifying taxonomy?." Nature Reviews Clinical Oncology 6 (12): 718-730.
4. Jensen E, H Jacobson (1962) Basic guides to the mechanism of estrogen action. Recent Progress in Hormone Research 18: 387-414.
5. Jensen E, GE Block, S Smith, K Kyser, ER DeSombre (1971) Estrogen receptors and breast cancer response to adrenalectomy. National Cancer Institute Monograph 34: 55-70.
6. Jones Kellie L, Aman U Buzdar (2004) A review of adjuvant hormonal therapy in breast cancer. Endocrine-related cancer 11 (3): 391-406.
7. Genant Harry K, J Lucas, S Weiss, M Akin, R Emkey, et al. (1997) Low-dose esterified estrogen therapy: effects on bone, plasma estradiol concentrations, endometrium, and lipid levels. Archives of internal medicine 157(22): 2609-2615.
8. Nelson Linda R, Serdar E Bulun (2001) Estrogen production and action. Journal of the American Academy of Dermatology 45(3): S116-S124.
9. Kuiper G, Carlsson B, Grandien K, E Enmark, J Haggblad, et al. (1997) Comparison of the ligand binding specificity and transcript tissue distribution of estrogen receptors ERα and β. Endocrinology 138(3): 863–870.
10. Torgov IV (1982) Synthesis of steroid hormones. Bulletin of the Academy of Sciences of the USSR, Division of chemical science 31(2): 271-284.
11. Celik, Leyla, Julie Davey Dalsgaard Lund, Birgit Schiøtt (2007) Conformational dynamics of the estrogen receptor α: molecular dynamics simulations of the influence of binding site structure on protein dynamics. Biochemistry 46(7): 1743-1758.
12. Shyamala G, W Schneider, M C Guiot (1991) Estrogen dependent regulation of estrogen receptor gene expression in normal mammary gland and its relationship to estrogenic sensitivity. Receptor 2(2): 121-128.
13. Shao Wenlin, Myles Brown (2004) Advances in estrogen receptor biology: prospects for improvements in targeted breast cancer therapy. Breast Cancer Research 6(1): 39-52.
14. Heldring Nina, Ashley Pike, Sandra Andersson, Jason Matthews, Guojun Cheng, et al. (2007) Estrogen receptors: how do they signal and what are their targets. Physiological Reviews 87(3): 905-931.
15. Nilsson Stefan, S Mäkelä, E Treuter, M Tujague, J Thomsen, et al. (2001) Mechanisms of estrogen action. Physiological Reviews 81(4): 1535-1565.
16. Savkur RS, TP Burris (2004) The coactivator LXXLL nuclear receptor recognition motif. The Journal of Peptide Research 63 (3): 207-212.
17. Brzozowski Andrzej M, AC Pike, Z Dauter, RE Hubbard, T Bonn, et al. (1997) Molecular basis of agonism and antagonism in the oestrogen receptor. Nature 389(6652): 753-758.
18. AC Pike, AM Brzozowski, J Walton, RE Hubbard, AG Thorsell, et al. (2001) Structural insights into the mode of action of a pure antiestrogen. Structure 9(2): 145-153.
19. Picard Didier (2006) Chaperoning steroid hormone action. Trends in Endocrinology & Metabolism 17(6): 229-235.
20. Ciocca Daniel R, Stuart K Calderwood (2005) Heat shock proteins in cancer: diagnostic, prognostic, predictive, and treatment implications. Cell Stress & Chaperones 10(2): 86-103.
21. Blagosklonny Mikhail V (2001) Re: Role of the heat shock response and molecular chaperones in oncogenesis and cell death. Journal of the National Cancer Institute 93(3): 239-240.
22. Mindi L Buckles (2014) Master of Science Thesis: Rotational Barrier Effects in a Unique Class of Estrogen Receptor Modulators, Florida Agricultural and Mechanical University.
23. Ho Bosco K, David A Agard (2009) Probing the flexibility of large conformational changes in protein structures through local perturbations. PLoS Computational Biology 5(4): e1000343.
24. Hockney RW, B Alder (1970) Methods in Computational Physics Alder B 136-211.
25. AK Shiau, D Barstad, PM Loria, L Cheng, PJ Kushner, et al. (1998) The structural basis of estrogen receptor/coactivator recognition and the antagonism of this interaction by tamoxifen. Cell 95 (7): 927-937.
26. Marino Maria, Paola Galluzzo, Paolo Ascenzi (2006) Estrogen signaling multiple pathways to impact gene transcription. Current Genomics 7(8): 497- 508.
27. (2014) OpenStax College. How Hormones Work. OpenStax-CNX, 26 June 2013 Web 05 April. *<http:// cnx.org/ content/ m44768/1.8/>*.
28. (2001) Version, "Sybyl 6.9", Tripos Associates, St Louis (MO).
29. Morris Garrett M, David S Goodsell, Robert S Halliday, Ruth Huey, William E, et al. (1998) Automated docking using a Lamarckian genetic algorithm and an empirical binding free energy function. Journal of Computational Chemistry 19(14): 1639-1662.